

CMB, SZ AND POLARIZATION SIMULATIONS FOR SOUTH POLE TELESCOPE AND E AND B EXPERIMENT.

CATHERINE LAFLAMME
August 2008

ABSTRACT

The South Pole Telescope (SPT) and the E and B Experiment (EBEX) are both experiments designed to analyse the cosmic microwave background, SPT to obtain information about the growth and development of galaxy clusters, and EBEX to analyze the few moments following the creation of the universe. More specifically, SPT analyses galaxy clusters in order to apply constraints on the equation of state to dark energy. EBEX, however, will focus on the polarization of the CMB, which has potential to be evidence of the current model of inflation.

These simulations were created as an efficient method to produce accurate and realistic data structures for both SPT and EBEX. The goal of the simulations is to provide analysers with known data, which will allow them to see directly, and then to understand the effects of processing the data. Then when dealing with real telescope data, the analysers will undoubtedly be in a much more confident position.

Subject headings:

1. SCIENTIFIC MOTIVATIONS

Since its discovery in 1965 (Penzel & Wilson et al. 1945) the cosmic microwave background (CMB) has been providing physicists with evidence which supports the Big Bang model, a model which describes the moments after the creation of the universe as a time of rapid inflation. As well the CMB provides information on the composition of the universe, namely the domination by dark energy. Experiments such as WMAP (WMAP et al. 2008) have already provided detailed information on large scale anisotropies of the CMB which allows for tight restraints on many of the cosmological parameters associated with this model. However there are questions that remain unanswered, and further investigation should be conducted to exploit the unique view that the CMB gives us of the early universe. Questions involving the nature of dark energy and the energy scales of inflation motivate many experiments which probe the universe at the moments when it began. Two methods that can be used to further investigate the CMB are to study the effects of the Sunyaev-Zeldovich (SZ) effect on the CMB at fine angular scales and to study the polarization of the CMB.

1.1. *SZ Effect*

The SZ effect is characterized when photons from the CMB pass through the gas surrounding a galaxy cluster. These photons undergo an inverse compton scatter, gaining energy from the highly energetic electrons. As shown in figure 1, the SZ leaves a footprint on the pattern of the CMB as either an area of increased high energy photons, or as an area which lacks low energy photons, depending on your observing frequency. In this way an image of the CMB can be seen as a map of high density galaxy clusters, with small areas of distinctly higher energy indicating a galaxy cluster. Sufficient knowledge of these clusters is crucial in understanding the early universe as their growth is critically dependent on their underlying cosmology, and importantly, this information can be used to investigate the nature of dark energy (South Pole Telescope et al. 2004).

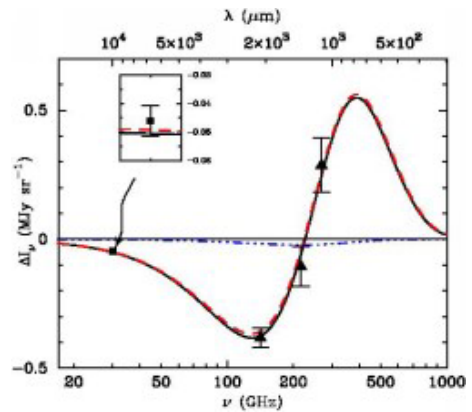


FIG. 1.— The Impact of the SZ effects on a photon from the CMB. The curve shows the difference in intensity of the CMB and the intensity of the CMB after it has passed through a galaxy cluster. One should note that the SZ effect creates an intensity decrement at frequencies lower than 220GHz and an intensity increment at higher frequencies.

1.2. *Polarization*

Detecting CMB polarization is a difficult task, as the signal is on the order of just several microKelvin, a level which presents significant challenges to experimentalists. However, the measurement of CMB polarization anisotropies would provide much needed information of our early universe. While temperature fluctuations may have evolved since the surface of last scattering (for example through the SZ effect) the photon polarization could not have been altered in any significant way. This gives us direct insight into the first moments of the universe. For this reason polarization is a powerful tool in unlocking the mystery of the beginning of the universe. Both density fluctuations and gravity waves present during the moments of inflation would result in Thomson scattering, (Hu & White et al. 1997) and therefore the linear polarization of photons. However there exists a distinction in the pattern of the induced polarization between these two sources, namely that density fluctuations result in a curl-free or E-mode polarization,

Flight	Duration (days)	Area (deg ²)	Det (#)	Det/band (#)	NEQ,U/band ($\mu\text{K}\sqrt{\text{sec}}$) ^a	NET/band ($\mu\text{K}\sqrt{\text{sec}}$) ^a	Q,U ($\mu\text{K}/\text{pix}$) ^a	T ($\mu\text{K}/\text{pix}$) ^a
LD	14	350	1406	(752, 376, 278)	(5.0, 14.5, 131)	(3.5, 10, 92)	0.63	0.45
NA	0.83	150	316	(94, 94, 128)	(14, 29, 192)	(10, 21, 136)	4.8	3.4
^a Thermodynamic units								

Center Frequency (GHz)	Band Width (GHz)	FWHM (arcminute)	NEQ,U/detector ($\mu\text{K}\sqrt{\text{sec}}$) ^a	NET/detector ($\mu\text{K}\sqrt{\text{sec}}$) ^a	Polarization Mod. Efficiency
153	40	8	136	96	99.0
252	71	8	282	199	99.8
408	84	8	2180	1538	98.0
^a Thermodynamic units					

FIG. 2.— Details of EBEX frequency bands

while gravity waves result in a curl or B-mode polarization (which could not possibly be produced by density fluctuations alone). Therefore, the measurement of B-mode polarization would be direct evidence of gravity waves, and consequently a direct evidence of inflation. (Carlstrom et al. 2003)

2. THE SOUTH POLE TELESCOPE

The South Pole Telescope is a 10m off-axis gregorian telescope situated at the NSF south pole research station. The telescope, which measures millimeter emissions, is primarily designed to map primary and secondary anisotropies in the cosmic microwave background on fine angular scales, ie. multipoles exceeding $l \sim 2000$. On these scales the largest contributor to the distortions of the CMB is the SZ Effect, thus SPT's first project is conducting a survey over ~ 4000 degrees for galaxy clusters (South Pole Telescope et al. 2004). As well, SPT plans in the future to be measuring temperature anisotropies of CMB polarization on all angular scales. The SPT receiver is a focal array consisting of 960 superconducting Transition Edge Sensor (TES) bolometers. These bolometers are grouped into 6 wedges, each with 180 bolometers. The wedges range over three frequency bands. By ranging over multiple bands we are able to separate and isolate different emission sources in our spectrum.

3. E AND B EXPERIMENT

The E and B Experiment is a long-duration balloon-borne experiment of a 1.5m aperture telescope designed to collect measurements of the intensity and polarization of the CMB. EBEX will be equipped with 1406 TES bolometers at the receiver which will operate at three frequency bands, centered on 150, 250 and 410 GHz respectively. Figure 2 above gives details on the frequency bands, and flight information taken from the EBEX NASA proposal submitted in April 2007 (EBEX et al. 2007). The TES bolometers are designed to only measure photon intensity, and thus cannot detect polarization when used alone. Discussed in more detail in section ??, polarimetry will be achieved by the use of a fixed grid placed in front of the bolometers (which allows through only one component of the polarized light) as well as a rotating half wave plate, placed at the cold aperture stop of the optical system (which

flips the component of polarized light we are measuring, without having to alter the direction of the grid).

4. POINTING INFORMATION

Knowing the pointing information of the telescope allows us to link one data point with a known, distinct point in the sky. Because both telescopes are an array of detectors, rather than one single detector the pointing information is stored in two parts: one being the distances of each detector from the designated main, or boresight, bolometer, and two the timestream of where the boresight is pointing on the sky. Putting these two together we can calculate where each detector is pointing, at each time.

4.1. SPT

The pointing for SPT is taken from an existing SPT data structure; reading in the real pointing stream for a 1 hr time period. This stream is saved as an IDL variable and used as the pointing of the center of the telescope array in my simulations. Bolometer offsets are read in a similar way from the same data structure. As previously mentioned, with these two pieces of information we are able to calculate where each bolometer is pointing in the sky, at all times in my simulated scan.

4.2. EBEX

The boresight pointing stream for EBEX is taken from c-code written and run by Sam Leach¹. This code returns

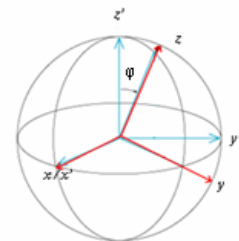


FIG. 3.— Two coordinate systems. Unprimed represents telescope coordinates characterized by az/el and primed representing the sky coordinates, characterized by ra/dec.

¹ Sam Leach, International School for Advanced Studies, Trieste, Italy

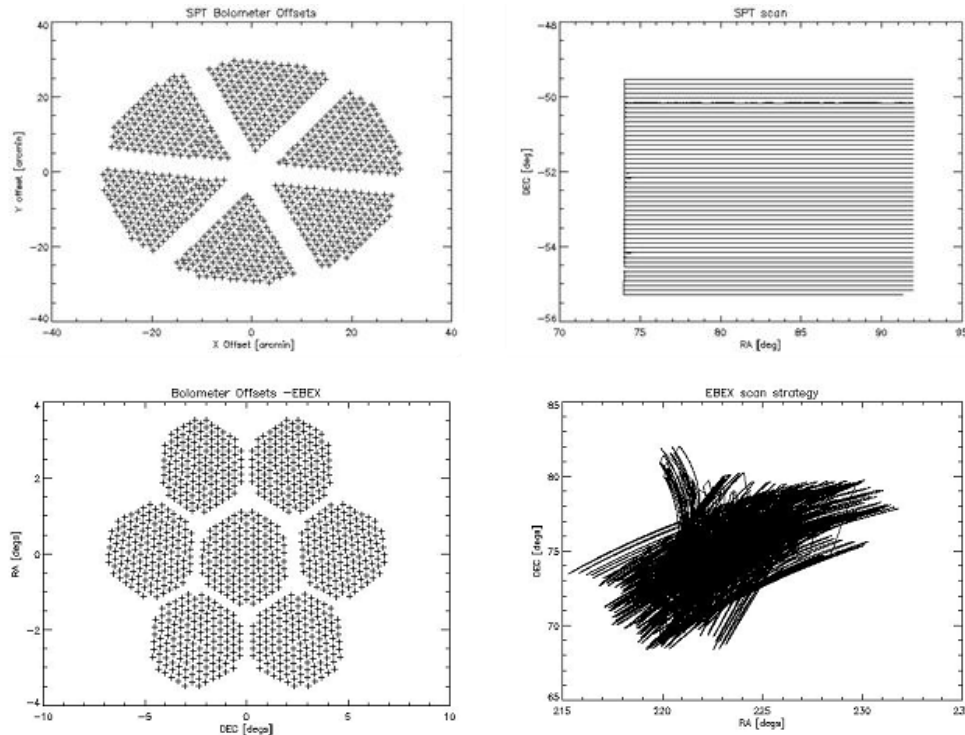


FIG. 4.— *Top Left* - Detector offsets in SPT. *Top Right* - An SPT scan strategy. *Bottom Left* - Detector offsets in Ebex. *Bottom Right* - An Ebex scan strategy.

streams of ra, dec and beta (the orientation of the focal plane of bolometers relative to the sky). This pointing information is a simulation of two hours of pointing data for a CMB scan, observing the beta-UMi region of sky from Fort Sumner, May 1 2009. The choice of this scan was inspired by the MAXIPOL observations ².

Bolometer offsets in EBEX are read in as differences in azimuth and elevation at the point [0,0] in the sky. However these offsets cannot be simply applied at every boresight pointing. We can see that this is true by considering the following example. Take a bolometer with an offset of purely azimuth, ie one that is at the same elevation as the boresight pointing. Now turn the boresight pointing to [0,90]. If we were to keep the original offsets, the bolometer in question would have no change in elevation, a change in AZ (would have no effect at the [0,90]) and would thus point at the exact same point in the sky.

To correct for this inconsistency, as the boresight moves through the sky I will rotate the offsets along the sphere, and then once at the final position, I will add the offsets to obtain individual bolometer pointing information.

This rotation is defined by the matrix R, and can be applied to the cartesian coordinates of the bolometers in the primed coordinate system.

$$R = \begin{pmatrix} \cos(\theta)\cos(\phi) & \sin(\phi) & -\cos(\phi)\sin(\theta) \\ \cos(\theta)\sin(\phi) & \cos(\phi) & -\sin(\theta)\sin(\phi) \\ \sin(\theta) & 0 & \cos(\theta) \end{pmatrix}$$

where $\theta = 90 - \text{dec}$ and $\phi = \text{ra}$ (of the boresight).

This rotation allows us to find the az/el pointing of each bolometer.

² <http://xxx.sissa.it/abs/astro-ph/0611394>

For convenience we would like to convert our coordinates into those of ra/dec.

In order to accomplish this we define two coordinate systems, shown in figure 3, unprimed which is characterized by az and alt, and primed which is characterized by ra and dec. The primed system rotates about z' at an angular velocity of $2\pi/\text{day}$. Because we are taking offsets, differences between points, this constant velocity has no effect on our measurements and can be negated. Z differs from Z' by an angle of $\psi = (90 - \text{latitude})$. We assume that $x = x'$.

With this notation, we can rotate between coordinate systems by the rotation matrix:

$$A = \begin{pmatrix} 1 & 0 & 0 \\ 0 & \cos(\psi) & \sin(\psi) \\ 0 & -\sin(\psi) & \cos(\psi) \end{pmatrix}$$

The first step in our transformation is to obtain cartesian coordinates of every bolometer. The center pixel is at: $[x_c, y_c, z_c] = [1, 0, 0]$ (corresponding to an az/el of (0,0)). Each bolometer's coordinates are then given by:

$$\begin{pmatrix} x_i \\ y_i \\ z_i \end{pmatrix} = \begin{pmatrix} \cos(\Delta az_i) \cos(\Delta el_i) + x_c \\ \sin(\Delta az_i) \cos(\Delta el_i) + y_c \\ \sin(\Delta el_i) + z_c \end{pmatrix}$$

The next step would be to transform these points into coordinates in the primed coordinate system. This transformation is characterized by:

$$\vec{x}' = A\vec{x} \quad (1)$$

Once we have the cartesian coordinates in the primed system we can find ra and dec by solving the trigonometric equation of spherical coordinates.

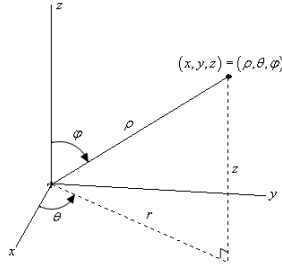


FIG. 5.— Spherical and Cartesian coordinates

$$\begin{aligned}\phi &= \arctan\left(\frac{y}{x}\right) \\ \theta &= \arctan\left(\frac{z}{\sqrt{(x)^2 + (y)^2}}\right) \\ \rho &= \sqrt{x^2 + y^2 + z^2}\end{aligned}$$

Applying these equations to our data we can obtain:

$$\begin{aligned}\Delta ra_i &= \arctan\left(\frac{y'_i - y'_c}{x'_i - x'_c}\right) \\ \Delta dec_i &= \arctan\left(\frac{z'_i - z'_c}{\sqrt{(x'_i - x'_c)^2 + (y'_i - y'_c)^2}}\right)\end{aligned}$$

The final step in obtaining the correct EBEX pointing information is to rotate the focal array by the parameter β . This allows one final degree of freedom for the array through the sky, and it simply describes another rotation. To apply this final rotation, each bolometer is rotated into a coordinate system where the focal array lies on the (new) x-y plane. Then a rotation by β can be described simply by the rotation:

$$A = \begin{pmatrix} \cos(\beta) & \sin(\beta) & 0 \\ -\sin(\beta) & \cos(\beta) & 0 \\ 0 & 0 & 1 \end{pmatrix}$$

Once these coordinates are rotated by beta, they are rotated back to the original frame, giving the final bolometer coordinates.

5. CREATING A CMB/ SZ IMAGE

The first step in my simulations is to create an image of the sky which would include temperature information of both the CMB and the SZ effect.

A CMB image can be created by first plotting the known power spectrum.³ Once we have a power spectrum we have the entire *magnitude* information in fourier space - but we are missing the phase information. By multiplying the spectrum by random (gaussian) complex numbers of magnitude 1 we are creating phases which follow a gaussian distribution. By transforming back to real space we obtain an accurate CMB image. This method of randomizing the phases of a power spectrum is efficient and very applicable, and will be used several more times in my simulations.

An image which includes information on the SZ effect is obtained by using the output fits files from the work

³ A spectrum of C_l values can be obtained by CMBfast which can be found at <http://cfa-www.harvard.edu/mzaldarr/CMBFAST/cmbfast.html>

done by Laurie Shaw⁴. His fits images are $\approx 5^\circ \times 5^\circ$ maps of the Y-parameter of this region of sky. The Y parameter is a representation of energy of a photon and is defined as:

$$y = \frac{\text{energy gain/scattering} \times \text{total number of scatterings}}{\text{scatterings}}$$

The y parameter can be converted into a temperature decrement by :

$$\Delta Y = y \left(e^{\frac{x}{2}} + 1 \right) T \quad (2)$$

where x is dimensionless and $= 2.6389866$ when measuring at 150 GHz (Schultz & White et al. 2002).

In order to create an image large enough to cover the SPT and EBEX scan strategies, these images are tiled in a checkerboard arrangement. After having converted the image to temperature units, it is smoothed the image with a gaussian with the full width half max pertaining to that of the beam size of the telescope. (1 arcminute - SPT, 8 arcminutes- EBEX). This is necessary as our beam maps a gaussian function, rather than a delta function in response to a point source. I use a program written by Michael Fogel⁵ to complete the convolving; a program based on the convolution theorem. This theorem states that the Fourier transform of a convolution is the product of their two respective transforms. To apply this theorem, the Fourier transform of my map is multiplied with the Fourier transform of a gaussian (also a gaussian) and then reverse transformed back into real space. This will result in a smoothed image.

5.1. Making a sky image timestream

Information of the pointing of the telescope and the completed sky image can be used to create telescope timestreams. The first task involved is to associate to each ra/dec coordinate, a corresponding pixel on my created sky image. This is accomplished by first centering the ra and dec by subtracting the median, then altering the ra by a factor of cosine the declination, to swith into square coordinates. Units of degrees are converted into pixels by applying the map resolution (which defines the map in terms of arcminutes on the edge of one pixel). To ensure that the scan is centered in the middle of the array rather than at the [0,0] pixel, the pixel mean is added to both the x and y coordinate. This results in a stream of telescope pointing in terms of pixel location on my sky image. The individual bolometer offsets, once scaled by the same map resolution constant as above can now be directly applied to this stream. These streams of x and y pixels are used to efficiently locate where in the sky image each bolometer is pointing. Taking the information stored at this pixel gives me a fast way to create accurate timestreams.

6. NOISE SIMULATIONS

The addition of noise in my simulations is crucial as noise is an unavoidable reality in any electrical system.

⁴ Laurie Shaw, McGill University, QC. For more information on his simulations see <http://adsabs.harvard.edu/abs/2007ApJ...663..139B>

⁵ Michael Fogel - Berkely CA

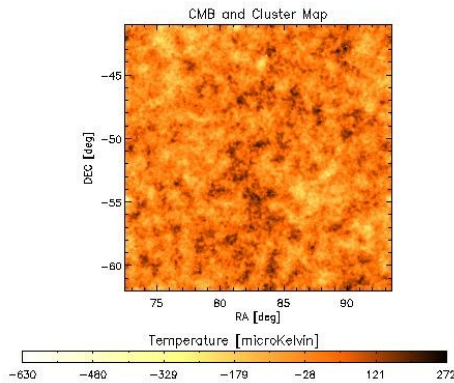


FIG. 6.— A Smoothed Sky Image

A stream of simulated noise is created through a code written by Micheal Fogel in 2004. This program constructs a power spectrum which includes white and $1/f$ noise, as well as a bolometer roll off and an electronic roll off. As done with the CMB image, the phases are then randomized, and then reverse fourier transformed back into real space, to obtain a noise timestream. This process is repeated for each bolometer.

6.1. $1/f$ noise

The power in the $1/f$ signal is contributed to by the atmosphere as well as electronic noise. The noise is characterized by a power spectrum which follows a $1/f$ curve in frequency space. A $1/f$ spectrum is characterized by it's *knee*, the frequency at which it's intensity matches that of white noise. For SPT we estimate the $1/f$ corner frequency to be at 1 Hz.

6.2. Bolometer Roll Off

When considering the array of bolometers, we must recognize the reality that heat can only be transferred at a finite time. There exists in our noise power spectrum a roll off as a result of this time constant inherent to the bolometers, which relates to how fast heat can be transferred throughout the bolometer web. This constant is given as $\tau = C/G$ where C is the heat capacity of the given bolometer and G is the thermal conductance of the link. For SPT we estimate this constant to be at 18 Hz.

6.3. Electronic Roll Off

The electronic roll off originates from the time constant associated with a low pass filter that we purposely impose on our signal post-detection. This filter allows for the attenuation of higher frequencies and ultimately determines the signal and noise bandwidth (Spieler et al. 2007). For SPT this roll off is set at 40 Hz.

7. ATMOSPHERIC FLUCTUATIONS FOR SPT

7.1. Obtaining an atmospheric image

The impact of the fluctuations in the atmosphere on a ground based telescope have been studied in detail and it has been shown that the observed atmospheric signal is characterized by the Kolmogorov-Taylor Model. This model describes the atmospheric power spectrum

and can be given as:

$$P(\alpha_x^2, \alpha_y^2) = \begin{cases} Ah_{av}^{5/3}(\alpha_x^2 + \alpha_y^2)^{-11/6} & \frac{h_{av}}{2\Delta h} \ll (\alpha_x^2 + \alpha_y^2)^2 \ll \alpha_i \\ Ah_{av}^{2/3}(\alpha_x^2 + \alpha_y^2)^{-8/6} & \alpha_o \ll (\alpha_x^2 + \alpha_y^2)^2 \ll \frac{h_{av}}{2\Delta h} \end{cases}$$

where Δh is the depth of the atmosphere layer, and h_{av} is the height of the layer from the telescope. A study conducted by R.S. Bussmann (Bussman et al. 2004) on the millimeter wavelength brightness fluctuations obtained median fluctuation power amplitudes of $10 \text{ mK}^2 \text{ rad}^{-5/3}$ in Rayleigh Jean temperature units. We are then just left to turn this spectrum into a 2-d image which is done by applying the FFT in two dimensions. After multiplying the spectrum by an array of random phases, we can FFT back into real space, to obtain a final image.

7.2. Smoothing the Atmosphere Image

For each of our telescopes we can model our beams using gaussian optics. Gaussian optics is a simple way of modeling radiation as a light bundle with a radial gaussian power distribution. A Gaussian model compromises between simplistic ray diagrams and the rigorous calculations of diffraction by taking into account only the first order diffraction effects.

A Guassian beam can be characterized by it's width, which can be described in two ways:

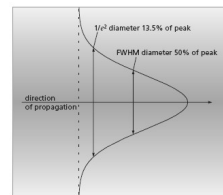


FIG. 7.— Two methods to characterize a Gaussian distribution

- $\frac{1}{e^2}$ width : the width of the distribution when the intensity falls to $\frac{1}{e^2} \approx 0.135$ of its maximum value.
- FWHM : the width of the distribution when the intensity falls to $\frac{1}{2}$ of its maximum value

We can convert between the two by the relation:

$$2 \ln(2) = \left(\frac{2 FWHM}{\frac{1}{e^2}} \right)^2 \quad (3)$$

While beam information is most commonly given in terms of the FWHM, for purposes of beam calculations it is more practical to work with $\frac{1}{e^2}$.

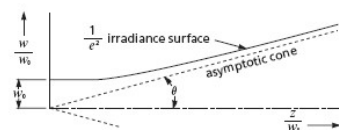


FIG. 8.— The $\frac{1}{e^2}$ Beam Radius as a function of distance from the waist - clearly split between the near field (very small slope) and the far field (linear). Note θ_{asym} which defines the far field.

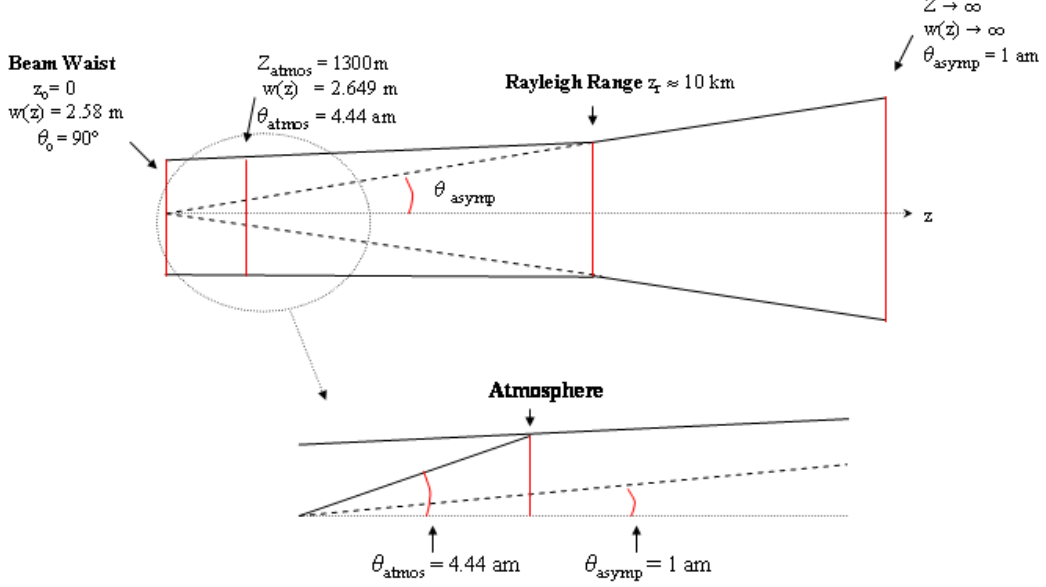


FIG. 9.— Beam Characteristics for SPT. Once in the far field, the beam width varies linearly by the angle θ_{asympt} . The atmosphere, which is present in the near field, has a beam width at an angle θ_{atmos}

It should be noted that the telescope beam radius, taken as a function of distance from the telescope cannot be characterized as one distinct function, and this must be taken into account when smoothing the resulting atmospheric image. In the far field limit (ie. the CMB, the SZ effect) the beam radius is a function of linear growth. This says that as we move farther from the beam source in distance, the beam radius (or beam width) increases proportionally. As shown in As we can see in figure 8, the angle of linear growth is called θ_{asympt} , and is the most common way of describing a beam. However, unlike the image of the CMB, the atmosphere is present in the near field. As we move out in distance from the telescope, the beam width no longer changes linearly. Applying the concepts of basic beam optics we will be able to find the beam radius at any point in this non-linear near field.

As we can see in figure 8 in the near field the beam radius, denoted by $\omega(z)$, diverges very slowly, while in the far field it asymptotes to a linear growth with z , at an angle θ_{asympt} . As previously mentioned, this angle, which is the $\frac{1}{e^2}$ width, fully characterizes the beam in the far field. Given a beam's FWHM in the far field we can find θ_{asympt} by applying the equation 3.

In the near field the $\frac{1}{e^2}$ beam radius is defined by the function:

$$\omega(z) = \omega_o \left(1 + \left(\frac{\lambda z}{\pi \omega_o^2} \right)^2 \right)^{\frac{1}{2}} \quad (4)$$

where ω_o is called the beam waist, and is defined as the minimum of the beam radius. Any radius is measured as a function of z , distance from this beam waist, where λ is the wavelength of light.

Because a beam is characterized by its FWHM in the far field we need a way to link between this parameter

and w_o the characterization of the beam in the near field. This relationship is given by:

$$\theta_{asympt} = \frac{\lambda}{\pi \omega_o} \quad (5)$$

The boundary at which the far field linear approximation holds is defined as the Rayleigh Range, and can be given as:

$$Z_r = \frac{\pi \omega_o^2}{\lambda} \quad (6)$$

7.2.1. Beam Characteristics for SPT

In SPT we use beams with a FWHM in the far field of 1 arcminute. By equation 3 this corresponds to an asymptotical angle, in the far field of:

$$\theta_{asympt} = 0.00247 \text{ radians}$$

and by equation (5) a beam waist (keeping in mind we are still measuring the width of the $1/e^2$ intensity) of:

$$\omega_o = 2.58 \text{ m}$$

The Rayleigh Range of the beam, given by equation 6 is:

$$Z_r = 10468.7 \text{ m}$$

Our simulated atmosphere, which is at a height of 1300 m is therefore well within near field, and using equation 4 we obtain the beam radius at this height as:

$$\begin{aligned} w(1300 \text{ m}) &= 2.649 \text{ m} \\ &= 4.44 \text{ arcminutes} \end{aligned}$$

Taking this beam radius as our new parameter, we can smooth the atmosphere images in the same method

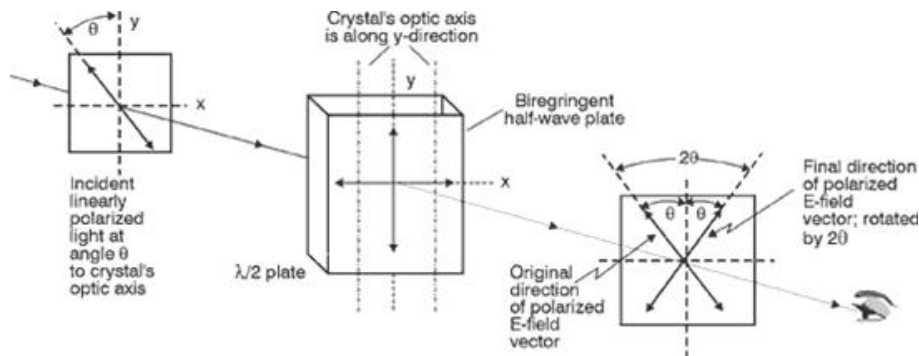


FIG. 10.— The effects of a Half Wave Plate

applied to the CMB image.

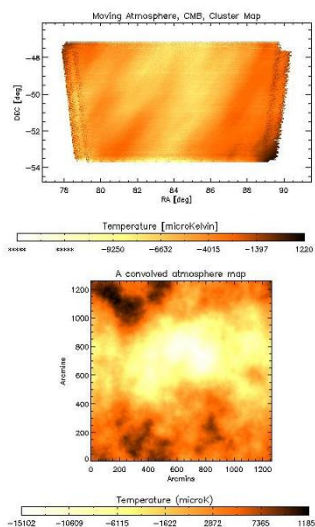


FIG. 11.— Two atmosphere maps: *Top* An atmosphere moving in both x and y. *Bottom* A static atmosphere.

7.3. Wind and Creating a timestream

Creating a timestream for the atmosphere uses an identical method as previously mentioned, with one slight alteration to account for wind. Making the assumption that the wind moves with constant velocity in x and y, (Bussman et al. 2004) we can use the distance of the atmosphere from the telescope, and map resolution to convert from a velocity in m/s to pixel/s. The subscripts on the atmosphere image as no longer constant and shift through time by these velocities.

8. MEASURING POLARIZATION

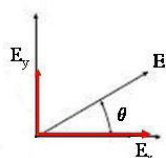


FIG. 12.— One possible linear polarization

EBEX will be using both a rotating half-wave plate

(HWP) and a fixed polarizing grid to measure the polarization signal. Already used by several experiments including the balloon borne experiment MAXIPOL, this technique has been proven to provide a strong discrimination against systematic errors. (EBEX et al. 2007)

8.1. Linear Polarization

When describing polarization it is sufficient to specify only the orientation of the electric field; the magnetic field will follow, because the vector is defined to be at 90° to both the E-field and the direction of propagation. When describing *unpolarized* light the instantaneous polarization fluctuates rapidly in a random manner. In *polarized* light we can accurately describe the light by the x-component and the y-component of the intensity of the E field. Any light can be characterized by a simple addition of its unpolarized and its polarized parts.

8.2. A Wave-Plate

A wave plate, or sometimes referred to as a retarder, is used to change the orientation of already linearly polarized light and will have therefore no effect on unpolarized light.

A wave plate typically works by first dividing an incident polarized beam into 2 components then changing the phase of one component relative to the other. The newly reconstructed beam now has a shifted polarization.

The question remains how do we shift the phase of only one component of light?

1. A typical waveplate is made of a birefringent crystal cut to a specific thickness.
2. This crystal is chosen specifically so that it has one axis of anisotropy (a direction dependent property). The refractive index, n , in the crystal is dependent on the orientation of light relative to this axis.
3. Because velocity of propagation through a medium is directly related to refractive index by the equation, $v_p = c/n$ for c the speed of light through a vacuum, by changing refractive index we change how quickly each component of the light is able to propagate.

Analysing (1) and (2) we can see that we now have the components of light moving at different speeds through the crystal, as a function of angle from the axis of anisotropy. The component of light aligned with this

axis is called the *fast-axis* and is said to pass through unattenuated. The light perpendicular to the fast axis is therefore slowed in relation to it, and by appropriately choosing the thickness of the crystal, we can retard the slow-component by exactly half a wavelength.

8.3. Jones Calculus

Jones calculus can be used in order to mathematically characterize the effects of a half wave plate to polarized light. A general expression of a plane harmonic wave is:

$$\begin{aligned} E &= E_x \hat{i} + E_y \hat{j} \\ &= |E_x| e^{i\phi_x} \hat{i} + |E_y| e^{i\phi_y} \hat{j} \end{aligned}$$

This can be represented by the Jones Matrix:

$$\begin{bmatrix} |E_x| e^{i\phi_x} \hat{i} \\ |E_y| e^{i\phi_y} \hat{j} \end{bmatrix}$$

This matrix can be normalized by taking out a factor of $(E_x^2 + E_y^2)^{\frac{1}{2}}$.

We can model linearly polarized light with an exclusively real vector. For example:

$$\begin{bmatrix} x \\ y \end{bmatrix}$$

represents linear polarization with the real components x and y . Circularly polarized light can be represented in a complex matrix, for example

$$\begin{bmatrix} 1 \\ i \end{bmatrix}$$

represents left circular polarization.

This provides a simple method to add light of different polarizations, we simply add their Jones vectors. A Jones matrix is a matrix representation of an optical element. When applied to the vector of incident light we will obtain the emerging light vector. For a half wave plate the Jones matrix can be written as:

$$T_{\text{HWP}} = \begin{bmatrix} -1 & 0 \\ 0 & 1 \end{bmatrix}$$

with the -1 representing the slow axis. We learn about the nature of the optical element by analysing the eigenvectors of the matrix. In the above case we have the eigenvectors of

$$\begin{bmatrix} 0 \\ 1 \end{bmatrix}$$

and

$$\begin{bmatrix} 1 \\ 0 \end{bmatrix}$$

with eigenvalues of 1 and -1 respectively. This is a mathematical representation of the observation that incident light which is strictly polarized in x or y will pass through unaffected when aligned with the fast axis, or will be phase shifted by 180° when completely aligned on the slow axis, as expected.

8.4. The Effect of Rotating the Wave Plate

By rotating the wave plate, we are rotating the fast and slow axis with respect to the stationary x and y axis.

For example, sending incident light of polarization $E_x = 0, E_y = 1$ would pass through the plate untouched. But after the plate has rotated a quarter of a cycle, according to the plate, the intensity E_y is now completely along the slow axis, and will be phase shifted.

We can compensate for this rotating coordinate system by applying a coordinate transformation to the vector of light before applying the wave-plate Jones Matrix. This matrix is simply given as:

$$P = \begin{bmatrix} \cos(\phi) & \sin(\phi) \\ -\sin(\phi) & \cos(\phi) \end{bmatrix}$$

where ϕ is the instantaneous displacement of the fast-axis from its origin. We now have all the tools to make a complete mathematical representation of the rotating HWP, in the form of a matrix, that can be easily programmed to be applied to a Jones vector of a photon. This matrix will transform into the coordinate system of the HWP, pass through the plate, then transforming back to the original frame. This matrix is given as:

$$\begin{aligned} T_{\text{rotHWP}} &= P_{\text{rot}}^{-1} T_{\text{HWP}} P_{\text{rot}} \\ &= \begin{bmatrix} \sin^2(\phi) - \cos^2(\phi) & -2\cos(\phi)\sin(\phi) \\ -2\cos(\phi)\sin(\phi) & \cos^2(\phi) - \sin^2(\phi) \end{bmatrix} \end{aligned}$$

8.5. Creating a timestream with a Half Wave Plate

Information on CMB polarization is obtained from the program *synfast*, a branch program of the Hierarchical Equal Area isoLatitude Pixelization (HEALpix).⁶ HEALpix is equipped with an IDL library including a procedure which reads in the output fits file into an IDL array variable. In addition there exists a procedure, which, given pointing vectors in *ra* and *dec*, will return the index of the associated pixel in this array. This allows for associating 3 stokes parameters, *I*, *Q*, and *U*, for any point in the sky. A procedure was created, with this procedure as a base, which associates to each bolometer at each time in the stream these parameters. Then, as an independent procedure, is a program which will takes as input, three stokes parameters and a time, will then take into account the position of the half wave plate at this time, and will return the intensity of the photon as observed through the fixed polarization grid. This procedure assumes the wave plate is spinning at a constant angular velocity, and uses jones calculus and coordinate rotations to find the resulting photon intensity. It saves only the component of light which runs flush to the direction of the fixed grid, as this is the only component of light detected by the telescope.

9. SIMULATION OUTPUT FORMATTING

In order that these simulations can be easily accessed by any collaborator in the group, they must be saved in the standard data format.

For SPT this is obtained by reading in an already created data structure, into an IDL variable. Simulated data can be added in by simply overwriting the bolometer timestream data with my own simulated timestreams.

⁶ see <http://healpix.jpl.nasa.gov/html/facilitiesnode11.htm>

By saving this overwritten data structure we have a properly formatted SPT data structure containing simulated data.

In EBEX the standard format for saving data is in a dir file. A dir file is essentially a collection of binary files, with a format file (a text file) describing the binary files. Using the IDL command binwrite, created timestreams can be stored as binary files. Then an existing format file is overwritten to include information of these timestreams.

10. SUMMARY

With the above software observations of both the South Pole Telescope and EBEX have been accurately simulated. Each timestream is given in the exact format that analysts receive real telescope data, and contains the information (such as noise, atmospheric effects etc...) that we expect to have an influence when analysing real telescope data. Using these simulations, analysts will be able to better understand their own software, providing in more accurate processing of real telescope data.

Already these simulations are being used by analysts at SPT to test their programs of common-mode removal, recovering sky signal from noise and atmosphere. Valuable knowledge has been gained, and analysts have been able to fine tune their programs to be at their best to analyze the real sky data. Soon analysts at EBEX will begin work in the same way with my simulations.

However, several aspects of the simulation can be improved upon. One major aspect that can be included is a program that will shuffle the incoming data. Realistic data coming in for EBEX will be in no logical order, and one problem analysts must overcome is to sort the timestreams into their proper order. Including this problem in my simulations would undoubtedly provide useful practice. Improvements in my simulations can as well be made to improve efficiency of the simulation pipeline in memory and time. These improvements include minimizing looping, by applying concepts of matrix algebra. In the future, further more subtle effects can be added to both timestreams, for example, adding the galactic dust effects.

11. ACKNOWLEDGEMENTS

I sincerely appreciate the time and help of:

Professor Matt Dobbs - *McGill University*

Professor Gil Holder - *McGill University*

Tijmen de Haan - *McGill University*

Laurie Shaw, Jon Dudley - *McGill University*

Sam Leach - *International School for Advanced Studies, Trieste, Italy*

Michael Milligan - *University of Minnesota*

William Grainger - *Columbia University*

REFERENCES

- [Penzel & Wilson et al. 1945]Penzias, A.A. & Wilson, R.J. 1945, *A Measure of Excess Antenna Temperature at 4080 Mc/s*
- [WMAP et al. 2008]Delabrouille,Cardoso, Le Jeune, Betoule, Fay, Guilloix 2008, *A Full Sky, low-foreground, High Resolution CMB map by WMAP*
- [South Pole Telescope et al. 2004]Ruhl, Ade, Carlstrom, Cho, Crawford, Dobbs, Greer, Halverson, Holzapfel, Lanting, Lee, Leong, Leitch, Lu, Leuter, Mehl, Meyer, Mohr, Padin, Plagge, Pryke, Schwan, Sharp, Runyan, Spieler, Staniszewski, Stark 2004, *The South Pole Telescope*
- [Hu & White et al. 1997]Hu, W. & White, M. 1997, *A CMB Polarization Primer*
- [Carlstrom et al. 2003]Carlstrom J.E., Kovac J., Leitch E.M, Pryke C, 2003, *Status of CMB Polarization Measurements from DASI and Other Experiments*
- [EBEX et al. 2007]2007, *Ebex Proposal to NASA*
- [Spieler et al. 2007]Spieler, H. 2007, *Bolometers and the Big Bang-Detector Arrays for Next Generation CMB Measurements*
- [Bussman et al. 2004]Bussman, R.S. & Holzapfel, W.L. & Kuo, C.L. 2004, *Millimeter Wavelength Brightness Fluctuations of the Atmosphere Above the South Pole*
- [Schultz & White et al. 2002]Schultz A.E., & White M. 2002, *Surveys of Galaxy Clusters with the Sunyaev Zel'dovich Effect*
- [Lay & Halverson et al. 2000]Lay, O.P. & Halverson, N.W. 2000, *The Impact of Atmospheric Fluctuations on Degree Scale Imaging of the Cosmic Microwave Background*
- [Fogel et al. 2004]Fogel,M.J. 2004, *APEX-SZ Observation Simulations*